The Prostaglandin D_2 Receptor CRTH2 Promotes IL-33–Induced ILC2 Accumulation in the Lung

Oyebola O. Oyesola,*,†,‡ Carolina Duque,*,† Linda C. Huang,*,† Elisabeth M. Larson,*,† Simon P. Früh,*,† Lauren M. Webb,*,†,‡ Seth A. Peng,*,† and Elia D. Tait Wojno*,†,‡

Group 2 innate lymphoid cells (ILC2s) are rare innate immune cells that accumulate in tissues during allergy and helminth infection, performing critical effector functions that drive type 2 inflammation. ILC2s express ST2, the receptor for the cytokine IL-33, and chemoattractant receptor-homologous molecule expressed on Th2 cells (CRTH2), a receptor for the bioactive lipid prostaglandin D_2 (PGD_2). The IL-33–ST2 and the PGD_2–CRTH2 pathways have both been implicated in promoting ILC2 accumulation during type 2 inflammation. However, whether these two pathways coordinate to regulate ILC2 population size in the tissue in vivo remains undefined. In this study, we show that ILC2 accumulation in the murine lung in response to systemic IL-33 treatment was partially dependent on CRTH2. This effect was not a result of reduced ILC2 proliferation, increased apoptosis or cell death, or differences in expression of the ST2 receptor in the absence of CRTH2. Rather, data from adoptive transfer studies suggested that defective accumulation of CRTH2-deficient ILC2s in response to IL-33 was due to altered ILC2 migration patterns. Whereas donor wild-type ILC2s preferentially accumulated in the lungs compared with CRTH2-deficient ILC2s following transfer into IL-33–treated recipients, wild-type and CRTH2-deficient ILC2s accumulated equally in the recipient mediastinal lymph node. These data suggest that CRTH2-dependent effects lie downstream of IL-33, directly affecting the migration of ILC2s into inflamed lung tissues. A better understanding of the complex interactions between the IL-33 and PGD_2–CRTH2 pathways that regulate ILC2 population size will be useful in understanding how these pathways could be targeted to treat diseases associated with type 2 inflammation. *The Journal of Immunology*, **2020, 204: 1001–1011.**

Group 2 innate lymphoid cells (ILC2s) are rare innate immune cells of the lymphoid lineage (lin) that are important mediators of type 2 inflammation during allergic disease and helminth infection (1–3). ILC2s do not express markers for T, B, and NK cells, or myeloid cell types but do express receptors for IL-33, IL-25, thymic stromal lymphopoietin, and the prostaglandin D_2 (PGD_2) receptor chemoattractant receptor-homologous molecule expressed on Th2 cells (CRTH2) (4–7). ILC2s are found in the lungs, intestine, skin, lymph nodes (LNs), blood, spleen, bone marrow (BM), and other tissues (1, 2, 8, 9) and are an important source of the type 2 cytokines IL-4, IL-5, IL-9, and IL-13 (2, 3). ILC2s increase in number at sites of allergic inflammation (10, 11) and during helminth infection (1, 8, 12). Some studies suggest that ILC2s are largely tissue-resident cells, seeded in the tissue early in life (8, 13, 14). Thus, such accumulation may be due to proliferation of ILC2s that are already in the tissue. However, other studies suggest that ILC2s can migrate into tissues from other sites during inflammation (6, 8, 15–19). The mechanisms and pathways that control ILC2 accumulation in tissues and the contribution of ILC2 migration into and between tissues during type 2 inflammation are not fully defined.

Various mediators act on ILC2s to promote their activation and proliferation during type 2 inflammation (20–22). IL-33 is an epithelial- and myeloid cell–derived cytokine that is released during type 2 inflammation (23–26). Previous studies have shown that exogenous IL-33 treatment can be used to model ILC2-associated allergic airway inflammation (10–13, 27). ILC2 accumulation in the lung in this model (10–13, 27) can be due to IL-33–induced ILC2 proliferation in the tissue (16, 28, 29), activation of pathways that promote the migration of ILC2 progenitors from the BM to the tissue site (16), or recirculation of ILC2s from other tissues sites (15).

Levels of bioactive lipids, such as PGD_2, are also elevated in type 2 inflammatory disease states (30–33). PGD_2 is an eicosanoid derived largely from dietary arachidonic acid via the action of cyclooxygenase (Cox) enzymes and hematopoietic PGD synthase (Hpgds) (34–36). During type 2 inflammation, PGD_2 is produced in response to an array of cues, with some in vitro evidence suggesting that epithelial cell–derived cytokines, such as IL-33, can induce PGD_2 synthesis and release (36, 37). PGD_2 is a ligand for the receptors DP1 and CRTH2. PGD_2 ligation of CRTH2 can

*Baker Institute for Animal Health, Cornell University College of Veterinary Medicine, Ithaca, NY 14850; †Department of Microbiology and Immunology, Cornell University College of Veterinary Medicine, Ithaca, NY 14850; and ‡Department of Immunology, University of Washington, Seattle, WA 98109

ORCIDs: 0000-0002-5347-7502 (O.O.O.); 0000-0003-3737-3858 (C.D.); 0000-0002-7582-3090 (L.C.H.); 0000-0001-9195-5061 (E.M.L.); 0000-0002-4757-8315 (S.P.F.); 0000-0003-2822-296X (E.D.T.W.).

Received for publication July 2, 2019. Accepted for publication December 5, 2019.

This work was supported by the National Institutes of Health, National Institute of Allergy and Infectious Diseases (grants K22 AI116729 and R01 AI130379 to E.D.T.W.) and Cornell University start-up funds (to E.D.T.W.). O.O.O. was the recipient of the Cornell African Fellowship and the Cornell Graduate Research Award. The content of this manuscript is solely the responsibility of the authors and does not necessarily represent the views of the National Institutes of Health.

Address correspondence and reprint requests to Dr. Elia D. Tait Wojno, University of Washington, Room E573, 750 Republican Street, Seattle, WA 98109. E-mail address: etwojno@uw.edu

The online version of this article contains supplemental material.

Abbreviations used in this article: BAL, bronchoalveolar lavage fluid; BFA, brefeldin A; BM, bone marrow; Cox, cyclooxygenase; CRTH2, chemoattractant receptor-homologous molecule expressed on Th2 cells; GMFI, geometric mean fluorescence intensity; Hpgds, hematopoietic PGD synthase; ILC2, group 2 innate lymphoid cell; IN, intranasal; lin, lineage; LN, lymph node; LSIG, lin$^-$Sca1^{hi}ID2^{hi}Gata3^{hi}KLRG1$^-$; MSLN, mediastinal LN; PAS, periodic acid–Schiff; PGD_2, prostaglandin D_2; rm, recombinant murine; WT, wild-type.

drive chemotaxis and/or increased type 2 cytokine production in vitro in type 2–associated immune cells, such as ILC2s, $CD4^+$ Th2 cells, eosinophils, basophils, and mast cells (6, 38–42). CRTH2 deficiency is associated with decreased pulmonary ILC2 accumulation after migratory helminth infection (6), but the role of the PGD_2–CRTH2 pathway in shaping ILC2 responses in vivo is not fully characterized. Critically, little is known about how cytokines, such as IL-33, influence PGD_2 production and how CRTH2-dependent effects control ILC2 activation in the tissue and migration into tissues in vivo.

Based on previous data connecting IL-33 to PGD_2 production and the importance of CRTH2 in controlling ILC2 accumulation in the lung (6, 36, 37), we hypothesized that IL-33–induced ILC2 accumulation in the lung is dependent on the PGD_2–CRTH2 pathway. To test this hypothesis, we treated wild-type (WT) and CRTH2-deficient (*Gpr44*$^{-/-}$) mice with exogenous recombinant murine (rm)IL-33 and examined ILC2 responses in the lung. We observed that rmIL-33 treatment resulted in upregulation of gene expression of the synthesis enzymes in the PGD_2 production pathway in WT and *Gpr44*$^{-/-}$ mice. Further, we observed a partial inhibition of rmIL-33–elicited ILC2 accumulation in the lung in CRTH2-deficient mice compared with WT mice, which was not a result of reduced proliferation or increased apoptosis or cell death of ILC2s. Rather, we found evidence that CRTH2 directly controlled ILC2 migration to the lung downstream of IL-33, as WT ILC2s preferentially accumulated in the lung compared with *Gpr44*$^{-/-}$ ILC2s following a 50:50 adoptive transfer into rmIL-33–treated recipient mice. Of note, the sizes of populations of transferred WT and *Gpr44*$^{-/-}$ ILC2s were not different in the draining mediastinal LN (MSLN). Together, these data suggest that ILC2 population size in the lung during type 2 inflammation was coordinated by IL-33 and the PGD_2–CRTH2 pathway, with IL-33 promoting ILC2 proliferation and increasing the capacity to produce PGD_2, which in turn regulated ILC2 migration patterns via CRTH2. An increased understanding of the networks of biochemical mediators that control ILC2 accumulation will inform the use and development of drugs that target these factors during type 2 inflammatory conditions, such as allergic disease and helminth infection.

Materials and Methods

Mice

Female C57BL/6 WT, CD45.1 C57BL/6 and Thy1.1 C57BL/6 mice were purchased from The Jackson Laboratory (Bar Harbor, ME) or bred in house. *Gpr44*$^{-/-}$ mice were provided by Amgen (Seattle, WA) and bred in house. All mice were used at 8–12 wk of age, and all experiments used age-matched controls. Animals were housed in specific pathogen–free conditions at the Cornell East Campus Research Facilities and/or the Baker Institute for Animal Health or the University of Washington South Lake Union 3.1 animal facility. WT and *Gpr44*$^{-/-}$ female mice were cohoused for 2 wk prior to experimental use. All experiments were performed under protocols approved by the Cornell University or the University of Washington Institutional Animal Care and Use Committees.

In vivo treatments, type 2 inflammation, and tissue preparation

Mice were treated intranasally (IN) or i.p. with 250 ng rmIL-33 (R&D Systems, Minneapolis, MN) or with 200 μl of PBS every other day for a total of three doses. Mice were euthanized on day 6 postinitiation of treatment. For *Nippostronglysus brasiliensis* infection, mice were infected s.c. with 500 L3 *N. brasiliensis* larvae maintained as described previously (43), and mice were euthanized at day 2 postinfection.

For all experiments, except where mentioned, the lungs were perfused through the apex of the heart before tissue collection. The middle, caudal, and accessory lobes of the lungs were collected for flow cytometry or cell sorting, and the cranial left and right lobes were collected for ELISA, RNA isolation, and histology. For flow cytometry and cell sorting, lungs were digested with 20 μg/ml DNase (Roche, Basel, Switzerland) and 2 mg/ml collagenase D (Roche) for 20–30 min at 37°C. BM was isolated by flushing one tibia and femur with cold RPMI 1640 (Corning, Corning, NY) with 1% L-glutamine (Corning). Single-cell suspensions of lung tissue, BM, MSLNs and mesenteric LNs were prepared by mashing the tissues individually through a 70-μm strainer. Lungs and BM were also RBC lysed with ACK lysis buffer (Lonza, Basel, Switzerland) for 1 min. For PBMC isolation, 0.3–0.5 ml of blood was collected with a glass pipette immediately after euthanasia into 100 μl of EDTA. PBMCs were isolated using a Ficoll-Paque (GE Healthcare, Uppsala, Sweden) gradient. Bronchoalveolar lavage fluid (BAL) was collected by instilling and recovering 1 ml of room temperature PBS (Corning) into the lung. The BAL was centrifuged at 1500 rpm for 5 min at 4°C, and the supernatant was stored at −80°C prior to analysis for cytokine levels.

For cell sorting, single-cell suspensions were prepared from tissues of female mice that had been treated i.p. every other day for 7 d with 5 ng rmIL-7 (R&D Systems) plus 30 μg anti-human IL-7 (Bio X Cell, West Lebanon, NH). On day 6 postinitiation of treatment, the lungs were collected and digested as described above.

Flow cytometry and cell sorting

Single-cell suspensions were incubated with Aqua LIVE/DEAD Fixable Dye (Thermo Fisher Scientific, Carlsbad, CA), and fluorochrome-conjugated mAbs against mouse CD3 (17A2), CD4 (GK1.5 or RM4-5), CD5 (53-7.3), CD11b (M1/70), CD11c (N418), CD19 (eBio1D3), CD25 (PC61.5), CD45 (30-F11), CD45.1 (A20), CD45.2 (104), CD127 (A7R34), CD90.2 (53-2.1 or 30-H12), CD90.1 (HIS51), CCR4 (2612), CD49d (R1-2), CXCR4 (2B11), IL-33R (RMST2-2), and/or NK1.1 (PK136) (from Thermo Fisher Scientific, BD Biosciences [San Jose, CA], or BioLegend [San Diego, CA]) for 30 min. For measuring apoptosis, cells were also stained with fluorochrome-conjugated annexin V (Thermo Fisher Scientific) in annexin binding buffer. For nuclear staining, cells were fixed using fixation/permeabilization buffer (Thermo Fisher Scientific), permeabilized using permeabilization buffer (Thermo Fisher Scientific), and stained with an mAb against Ki67 (B56) from BD Biosciences. For intracellular staining, cells were incubated for 4–6 h with 10 mg/ml brefeldin A (BFA) from Sigma-Aldrich (St. Louis, MO). Cells were then fixed in 2% PFA, permeabilized using BD Perm/Wash buffer (BD Biosciences) according to the manufacturer's instructions and stained with mAbs against IL-13 (eBio13A) and IL-5 (TRFK5). Samples were run on a three- or four-laser LSR II (BD Biosciences), a four-laser Attune NxT (Thermo Fisher Scientific), or a three-laser Gallios (Beckman Coulter, Brea, CA) flow cytometer and analyzed using FlowJo 10 (Tree Star, Ashland, OR).

For cell sorting, single-cell suspensions were incubated with Aqua LIVE/DEAD Fixable Dye (Thermo Fisher Scientific) and with fluorochrome-conjugated mAbs against mouse CD3 (17A2), CD5 (53-7.3), CD11b (M1/70), CD11c (N418), CD19(eBio1D3), CD45.1 (A20), CD127 (A7R34), CD90.2 (53-2.1), IL-33R (RMST2-2), and NK1.1 (PK136) (from Thermo Fisher Scientific or BioLegend) for 30 min. Fully stained cells were filtered through a 40-μM filter. ILC2s were gated as live, $CD45^+$, lin (CD3/CD5/CD11b/CD11c/CD19/NK1.1)$^-$$CD90.2^+CD127^+IL\text{-}33R^+$ (sometimes including CD25 as a marker as well) and sorted using a four-laser FACSAria Fusion (BD Biosciences) with an 85-μm nozzle.

In vitro culture

A total of 5×10^3 sorted lung ILC2s per well from mice treated with rmIL-7 plus anti-human IL-7 were cultured at 37°C and 5% CO_2 in DMEM (Corning) with 10% FBS (Corning), 1% L-glutamine (Corning), 1% penicillin/streptomycin (Corning), 25 mM HEPES buffer (Corning), and 55 μM 2-ME (Sigma-Aldrich) with 10 ng/ml rmIL-2 (Thermo Fisher Scientific), 10 ng/ml rmIL-7 (R&D Systems), and either 30 ng/ml rmIL-33 (R&D Systems), 100 nmol/ml PGD_2 (Cayman Chemical, Ann Arbor, MI), rmIL-33 plus PGD_2, or rmIL-33 plus PGD_2 plus the CRTH2-specific inhibitor OC000459 (1 μM) (44). PGD_2 and OC000459 were dissolved in 100 μl DMSO diluted 1:1000 in PBS. Equal volumes of DMSO were added to all the other treatments as a control. On day 3 and 5 of culture, fresh cytokines were spiked into cultures. On day 6, cells were analyzed by flow cytometry.

Real-time PCR

Total lung mRNA was isolated using TRIzol Reagent (Thermo Fisher Scientific), according to the manufacturer's protocol. For MSLNs, mRNA was isolated from pelleted cells from single-cell suspensions using the Norgen Single Cell RNA Purification Kit (Thorold, Ontario, Canada) according to the manufacturer's protocol. cDNA was generated using a Superscript II Reverse Transcriptase kit (Thermo Fisher Scientific), and real-time PCR was performed using SYBR Green Master Mix (Thermo Fisher Scientific) and commercially available primer sets (QIAGEN Quantitect Primer Assay; QIAGEN, Germantown, MD). Samples were

run on the Applied Biosystems 7500 or the Applied Biosystems ViiA 7 real-time PCR system (Thermo Fisher Scientific).

Adoptive cell transfer

Single-cell suspensions were prepared from the MSLNs of congenically marked WT or *Gpr44*$^{-/-}$ donor mice that were treated i.p. with 250 ng rmIL-33 (R&D Systems) every other day for a total of three doses and were euthanized on day 6 postinitiation of treatment. A total of 4×10^5 immune cells were combined in a 50:50 equal ratio and adoptively transferred i.p. into each recipient mouse that was pretreated with either PBS or rmIL-33. At day 6 postinitiation of treatment, the percentage and genotype of donor ILC2s and CD4$^+$ T cells in the blood, lungs, and MSLNs were determined by flow cytometry.

Histology

At necropsy, the left lung lobe was inflated with and stored in 4% PFA. Tissues were paraffin embedded, and 5-μm sections were stained with periodic acid–Schiff (PAS)/Alcian blue. Image acquisition was performed using a ZEISS AxioObserver Z1 Carl ZEISS Axio Camera and ZEISS ZEN Microscope acquisition software (ZEISS, Oberkochen, Germany) with 5× and 20× objectives. Adobe Photoshop (Adobe Systems, San Jose, CA) was used to adjust brightness, contrast, and color balance (changes were applied to the entirety of all images equally). Blind scoring was performed. Goblet cell scoring reflects presence and distribution of goblet cells in bronchial epithelium (1–5). Histology scoring reflects expansion of bronchial-associated lymphoid tissues (1–5), lymphoid infiltration around the blood vessels (1–5), number of submucosa glands (1–5), and accumulation of macrophages/multinucleated giant cells (1–5). These scores were added and averaged on a per sample basis.

Statistics

Statistical analysis was carried out using JMP software (SAS, Cary, NC). Sample size was determined per group by running a power analysis on preliminary or similar data sets using JMP 15 software ($\alpha = 0.05$, power = 0.8). For some readouts, variability and SD is higher than for others, and thus the number *n* required to achieve the specified power can differ between readouts. Data were analyzed using linear mixed effects models with a fixed effect of experimental group and a random effect of experiment day using JMP 15 software. Model assumptions of normality and homogeneous variance were assessed by a visual analysis of the raw data and the model residuals. Right-skewed data were log or square root transformed as indicated by the residuals. The experimental group was considered statistically significant if the fixed effect F test *p* value was ≤0.05. Post hoc pairwise comparisons between experimental groups were made using the Tukey honestly significant difference multiple-comparison test. Statistical outliers were identified using the extreme studentized deviate method and were omitted before performing the mixed model analysis. Graphs of results were shown as mean ± SEM of untransformed data using Prism version 7 (GraphPad Software, San Diego, CA).

Results

IL-33 induces expression of enzymes in the PGD_2 synthesis cascade

We first sought to determine whether IL-33–elicited type 2 inflammation is associated with an increase in the expression of enzymatic machinery for PGD_2 production in vivo. Employing rmIL-33–induced models of type 2 inflammation, in which mice were treated either i.p. or IN with rmIL-33 three times every other day (Fig. 1A), we measured gene expression of enzymes in the PGD_2 synthesis cascade, including genes that encode for phospholipase A2, Cox2, and Hpgds (34, 35), in the lungs and MSLN of rmIL-33– and PBS-treated WT and *Gpr44*$^{-/-}$ mice. We observed that i.p. or IN rmIL-33 treatment compared with PBS induced a significant increase in expression levels of *Pla2*, no statistically significant increase in *Cox2* expression, and a statistically significant increase in *Hpgds* expression in the lung of both WT and *Gpr44*$^{-/-}$ mice (Fig. 1B, 1C). Similar findings were observed in the MSLN (Supplemental Fig. 1A, 1B). These data suggest that rmIL-33 treatment is associated with an increase in gene expression for some players in the PGD_2 synthesis pathway, possibly increasing the capacity to produce PGD_2.

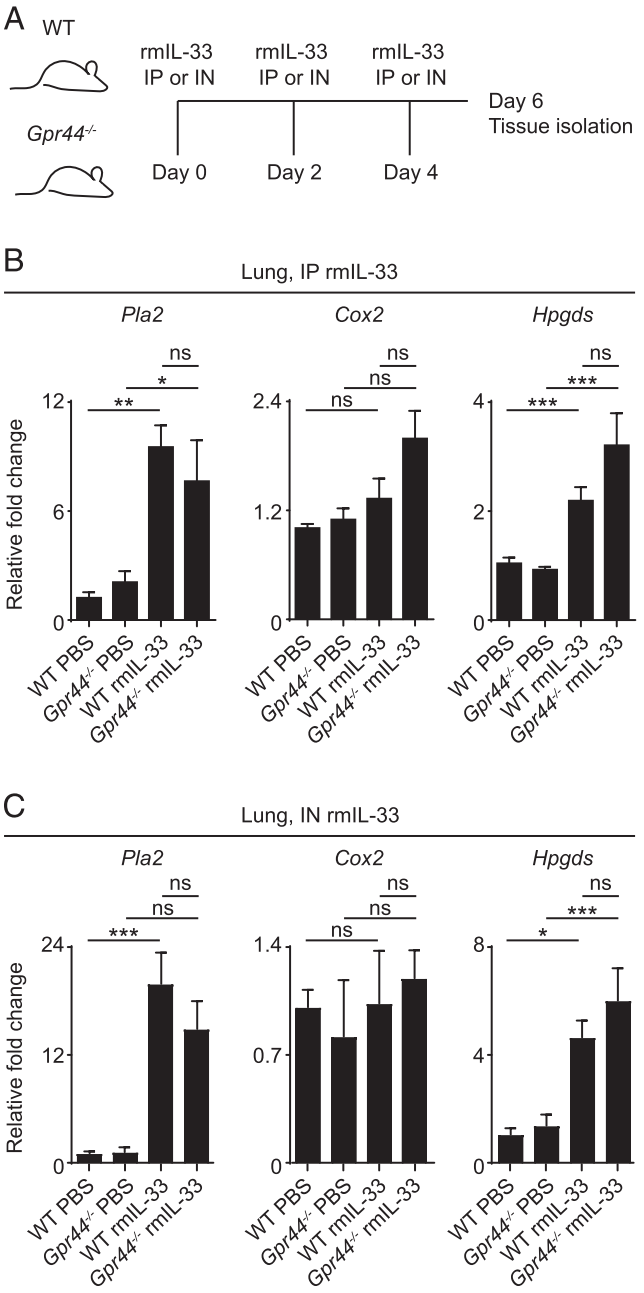

FIGURE 1. IL-33 induces expression of enzymes in the PGD_2 synthesis cascade in vivo. (**A**) C57BL/6 WT and CRTH2-deficient (*Gpr44*$^{-/-}$) mice were treated i.p. or IN three times with 250 ng of rmIL-33 or PBS every other day. On day 6 posttreatment initiation, mice were euthanized, and tissues were collected. Real-time PCR from total lung homogenate was used to measure expression of genes that encode phospholipase A2 (*Pla2*), *Cox2*, and *Hpgds*, all relative to *Actβ* and normalized to WT treated with PBS following (**B**) i.p. or (**C**) IN rmIL-33 treatment. Data are mean ± SEM, analyzed using a linear fixed effect model with pairwise comparison, compiled from two to five independent experiments; (B) PBS (n = 7–9), rmIL-33 (n = 12–16); (C) PBS (n = 3–4) or rmIL-33 (n = 5–6). $^*p \le 0.05$, $^{**}p \le 0.01$, $^{***}p \le 0.01$.

Lung ILC2 accumulation is partially CRTH2 dependent following multiple systemic rmIL-33 treatments

Upregulation of expression of genes in the PGD_2 synthesis pathway following rmIL-33 treatment suggested that IL-33–induced accumulation of ILC2s might be partially mediated by the PGD_2–CRTH2 pathway. To test this hypothesis, we assessed the frequencies and total number of ILC2s in the lung, identified

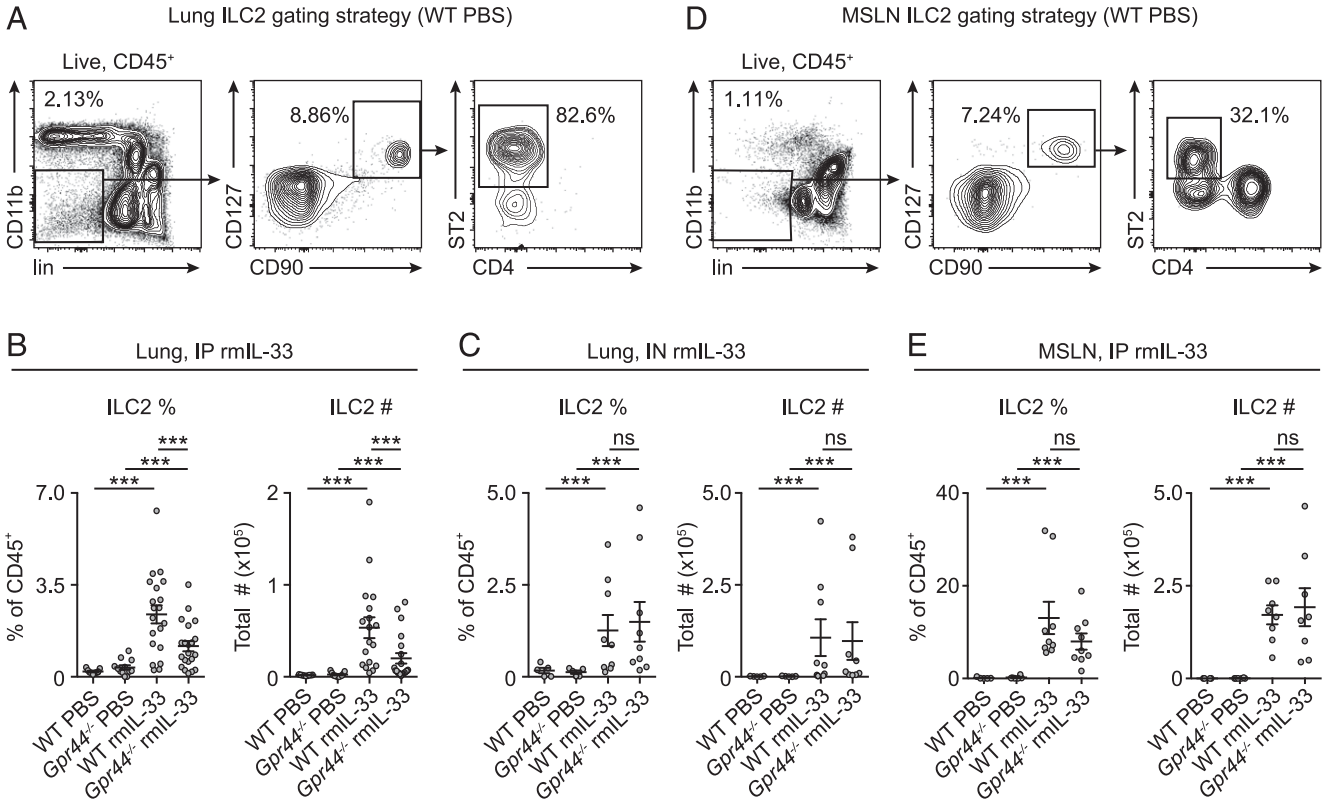

FIGURE 2. ILC2 accumulation in the lung is dependent on CRTH2 following multiple systemic treatments with rmIL-33. C57BL/6 WT and CRTH2-deficient (*Gpr44*$^{-/-}$) mice were treated i.p. or IN three times with 250 ng of rmIL-33 or PBS every other day. On day 6 posttreatment initiation, mice were euthanized, and tissues were collected. (**A**) ILC2s in the middle, caudal, and accessory lobes of the lung were gated as live, CD45$^+$lin(CD3/CD5/CD11c/CD19/NK1.1)$^-$CD11b$^-$CD90$^+$CD127$^+$CD4$^-$ST2$^+$. ILC2 percentage of CD45$^+$ cells and total ILC2 number in the lung following (**B**) systemic i.p. treatment and (**C**) local IN treatment. (**D**) ILC2s in the MSLN were gated as live$^+$, CD45$^+$lin$^-$CD11b$^-$CD90$^+$CD127$^+$ST2$^+$. (**E**) ILC2 percentage of CD45$^+$ cells and total ILC2 number in the MSLN following i.p. treatment. Data are mean ± SEM, analyzed using a linear fixed effect model with pairwise comparison; (B) data represent eight independent experiments or (C and E) three independent experiments; (B) PBS (n = 9–11), rmIL-33 (n = 17–20); (C) PBS (n = 5), rmIL-33 (n = 9); (E) PBS (n = 4–6), rmIL-33 (n = 8–9). ***$p \leq 0.001$.

as live, CD45$^+$lin$^-$CD11b$^-$CD90$^+$CD127$^+$ST2$^+$CD4$^-$ cells (Fig. 2A), in WT and *Gpr44*$^{-/-}$ mice following multiple systemic (i.p.) rmIL-33 treatments (Fig. 1A). The frequency of CD45$^+$ and total number of ILC2s increased in the lungs of WT mice treated with rmIL-33 compared with WT mice treated with PBS (Fig. 2B). This IL-33–elicited ILC2 accumulation in the lung was significantly reduced in *Gpr44*$^{-/-}$ compared with WT mice (Fig. 2B). There was no difference in rmIL-33–induced ILC2 accumulation in the lungs between WT and *Gpr44*$^{-/-}$ mice when rmIL-33 was delivered locally through IN administration (Fig. 2C), supporting previous studies suggesting that ILC2s do not recirculate through the blood following intratracheal IL-33 administration (13). Reduced ILC2 population size in *Gpr44*$^{-/-}$ compared with WT mice following multiple i.p. rmIL-33 treatments was also observed in the blood and mesenteric LNs (Supplemental Fig. 1C–F). Notably, the CRTH2-dependent ILC2 accumulation in the lung after multiple i.p. rmIL-33 treatments was cell type specific, as other cell types that express ST2 and/or CRTH2, such as eosinophils and CD4$^+$ Th2 cells (20, 39, 45, 46), accumulated equally in the lung in response to ongoing rmIL-33 i.p. treatment (Supplemental Fig. 1G–I). Strikingly, there was no difference in the lung-draining MSLN ILC2 (Fig. 2D) frequency and total number in response to multiple systemic treatments with rmIL-33 in WT and *Gpr44*$^{-/-}$ mice (Fig. 2E).

These experiments used multiple treatments with rmIL-33 and ongoing stimulation. However, IL-33 is also released during acute lung injury, including during *N. brasilensis* infection (26). To determine how CRTH2 might affect acute IL-33–elicited ILC2 accumulation, we compared pulmonary ILC2 accumulation in WT and *Gpr44*$^{-/-}$ mice 2 d after *N. brasiliensis* infection or 2 d after a single dose of i.p. rmIL-33. Two days postinfection with 500 larvae of *N. brasiliensis* (Supplemental Fig. 2A), there was an increase in the total numbers of ILC2s in the lungs and blood that was not significantly different between WT and *Gpr44*$^{-/-}$ mice (Supplemental Fig. 2B, 2C). Similarly, following a single dose of i.p. rmIL-33 (Supplemental Fig. 2D), there was an increase in the total number of ILC2s in the lung that was not different between WT and *Gpr44*$^{-/-}$ mice (Supplemental Fig. 2E). Taken together, these data suggest that CRTH2 partially yet specifically mediates IL-33–elicited lung ILC2 accumulation during systemic, ongoing type 2 inflammation but does not affect ILC2 accumulation in the lung-draining LN or during acute or local expansion of resident ILC2s in the lungs.

CRTH2 regulates IL-33–induced IL-5 production and type 2 inflammation in the lung but not ILC2-intrinsic cytokine production

The PGD_2–CRTH2 pathway has been implicated in the regulation of ILC2 population size (6) as well as ILC2 functions that promote type 2 inflammation (4). Therefore, we next tested whether type 2 cytokine levels and other parameters of type 2 inflammation associated with ILC2 responses that were elicited in the lung during ongoing IL-33 stimulation were CRTH2 dependent. Following multiple i.p. rmIL-33 treatments, IL-33–induced

gene expression of *Il5* but not *Il13* in the total lung homogenate was significantly downregulated in *Gpr44*$^{-/-}$ compared with WT mice, as assessed using real-time PCR (Fig. 3A). Likewise, IL-33–elicited increases in IL-5 protein levels were decreased in the BAL in *Gpr44*$^{-/-}$ compared with WT mice, and an IL-33–elicited upregulation in IL-13 levels in the BAL was not detectable at this time point (Fig. 3B). In addition, analysis of histological sections of the lung stained with PAS/Alcian blue revealed that type 2 inflammatory goblet cell hyperplasia, expansion of bronchial-associated lymphoid tissues, edema, and immune cell infiltration around the blood vessels were reduced in *Gpr44*$^{-/-}$ compared with WT mice following systemic IL-33 treatment (Fig. 3C, 3D).

The defect in global IL-33–elicited *Il5* and IL-5 levels in the lung and BAL of *Grp44*$^{-/-}$ mice suggested that the PGD_2–CRTH2 pathway might regulate ILC2 cytokine production following IL-33 exposure. To test this, we assessed spontaneous IL-5 and IL-13 production by ILC2s from WT and *Grp44*$^{-/-}$ mice following i.p. rmIL-33 treatment ex vivo by intracellular cytokine staining. A small percentage of lung ILC2s were single IL-5 producers in PBS-treated mice, and this population decreased and was replaced by IL-13 single producers in i.p. rmIL-33–treated mice, with similar patterns observed in WT and *Gpr44*$^{-/-}$ mice (Fig. 3E, 3F) as gated using isotype controls (Supplemental Fig. 3A). These data are in accord with recent single-cell transcriptional data from activated ILC2s (47). Similarly, sort-purified lung ILC2s from mice treated with rmIL-7 plus anti–IL-7 mAb complexes (which do not promote significant cytokine production) demonstrated significant spontaneous production of IL-5 and IL-13 in response to IL-33 stimulation in vitro, which was slightly but not strongly affected by the presence of PGD_2 with or without the CRTH2 inhibitor OC000459 (Fig. 3G, 3H). Although we observed distinct differences in ILC2 cytokine production patterns in response to IL-33 stimulation in vivo versus ex vivo, the PGD_2–CRTH2 pathway did not appear to significantly affect these responses. These results suggest that decreased parameters of type 2 inflammation in the lungs of *Gpr44*$^{-/-}$ mice relative to WT mice following ongoing i.p. rmIL-33 stimulation could be a result of decreased accumulation of ILC2s (Fig. 2B) rather than a direct influence of the PGD_2–CRTH2 pathway on IL-33–elicited ILC2 cytokine production.

Altered ILC2 accumulation in CRTH2-deficient mice following multiple i.p. rmIL-33 treatments is not a result of reduced ILC2 proliferation or increased apoptosis

Various mechanisms, such as cellular proliferation, cell death, apoptosis, and migration, can control the population size of cell types in tissues during inflammation (48). Some studies have suggested that ILC2 accumulation in tissues is largely because of expansion of the tissue-resident population (8, 13). Thus, we next tested whether CRTH2-dependent differences in ILC2 proliferation, apoptosis, cell death, or responsiveness to IL-33 proliferation or survival signals via ST2 expression were responsible for the impaired ILC2 population expansion elicited by multiple i.p. rmIL-33 treatments in *Gpr44*$^{-/-}$ compared with WT mice, assessed by measuring ILC2 Ki-67, annexin V, and LIVE/DEAD viability dye staining. Multiple i.p. rmIL-33 treatments elicited an increase in the frequency of Ki-67$^+$ lung ILC2s that was similar in WT and *Gpr44*$^{-/-}$ mice (Fig. 4A). Similarly, although there were lower frequencies of annexin V$^+$ and dead ILC2s in the lungs of WT and *Gpr44*$^{-/-}$ mice following rmIL-33 treatment (Fig. 4B, 4C), there were no differences between rmIL-33–elicited frequencies of annexin V$^+$ or dead ILC2s in the lung between WT and *Gpr44*$^{-/-}$ mice (Fig. 4B, 4C). In addition, whereas there was an rmIL-33–elicited increase of ST2 expression in lung ILC2s, this induction was not significantly different between WT and *Gpr44*$^{-/-}$ mice (Fig. 4D, 4E). These studies suggest that the partial abrogation of ongoing i.p. rmIL-33–induced ILC2 accumulation in *Gpr44*$^{-/-}$ mice (Fig. 2) is not likely because of reduced proliferation, increased apoptosis or cell death, or differences between in ST2 expression between WT and *Gpr44*$^{-/-}$ mice but, rather, may be mediated by altered ILC2 migration to or retention in the lungs of *Gpr44*$^{-/-}$ mice.

CRTH2-dependent ILC2 accumulation following multiple i.p. rmIL-33 treatments is not mediated via changes in ILC2 integrin or chemokine receptor expression

Whereas previous studies have suggested a direct role for PGD_2 in the regulation of ILC2 chemotaxis, especially in vitro (6, 40, 42), it is also possible that PGD_2 signaling through CRTH2 on ILC2s indirectly regulates the ability of ILC2s to home to or be retained in tissues by upregulating ILC2 expression of integrins and chemokine receptors (16, 17, 49–52). These include αβ integrins, such as CD18 and CD49d, selectins, such as CD62L, and chemokine receptors, such as CCR4 and CXCR4 (13, 17, 52, 53). Therefore, we tested whether CRTH2 regulates expression of CD49d, CD18, CD62L, CCR4, or CXCR4 on ILC2s isolated from lungs of WT and *Gpr44*$^{-/-}$ mice given multiple i.p. PBS or rmIL-33 treatments. In concert with previous findings (17), rmIL-33 led to increased ILC2 expression of the β1 integrin CD49d, quantified by the percentage of positive ILC2s and geometric mean fluorescence intensity (GMFI), that was similar in WT and *Gpr44*$^{-/-}$ mice (Supplemental Fig. 3B). Most lung ILC2s were positive for CD18, a component of the β_2 integrin, in both in PBS- and rmIL-33–treated WT and *Gpr44*$^{-/-}$ mice (Supplemental Fig. 3C). Multiple i.p. rmIL-33 treatments did not influence expression of CD62L on lung ILC2s in WT or *Gpr44*$^{-/-}$ mice (Supplemental Fig. 3D). Consistent with data showing that chemokine receptor expression can be regulated by IL-33 (13), multiple i.p. rmIL-33 treatments, compared with PBS, induced an increase in the percentage of CCR4$^+$ and CXCR4$^+$ lung ILC2s and CCR4 and CXCR4 GMFI in WT and *Gpr44*$^{-/-}$ mice (Supplemental Fig. 3E, 3F). There was no significant difference in this effect between WT and *Gpr44*$^{-/-}$ mice, except in the case of a decreased rmIL-33–elicited percentage of CXCR4$^+$ ILC2s in the lungs of *Gpr44*$^{-/-}$ compared with WT mice (Supplemental Fig. 3F). In addition, there were no significant differences in rmIL-33–elicited expression of the genes encoding the associated chemokine ligands CCL17, CCL22, and CXCL12 (50, 54) in WT and *Gpr44*$^{-/-}$ mice (Supplemental Fig. 3G). Taken together, these data suggest that ongoing i.p. rmIL-33–elicited ILC2 lung accumulation that is partially dependent on CRTH2 is not due to CRTH2-mediated changes in ILC2 integrin or chemokine receptor expression.

CRTH2 regulates the proportion and number of matured ILC2s in the BM following multiple i.p. rmIL-33 treatments

Previous studies have identified the BM as a potential source of adult ILC2s (8, 14, 16). To understand the influence of CRTH2 on maturation and kinetics of migration of ILC2 following prolonged systemic IL-33 stimulation, we assessed the percentage of ILC2 precursors and matured differentiated cells, identified as lin$^-$Sca1^{hi}ID2^{hi}Gata3^{hi}KLRG1$^-$ (LSIG) and KLRG1$^+$ LSIG, respectively (55, 56) (Fig. 5A), in the BM in WT and *Gpr44*$^{-/-}$ mice following prolonged systemic administration of rmIL-33. There was no difference in the percentage and number of ILC2Ps in the BM following prolonged systemic IL-33 stimulation compared with PBS in WT mice (Fig. 5B). This is in concert

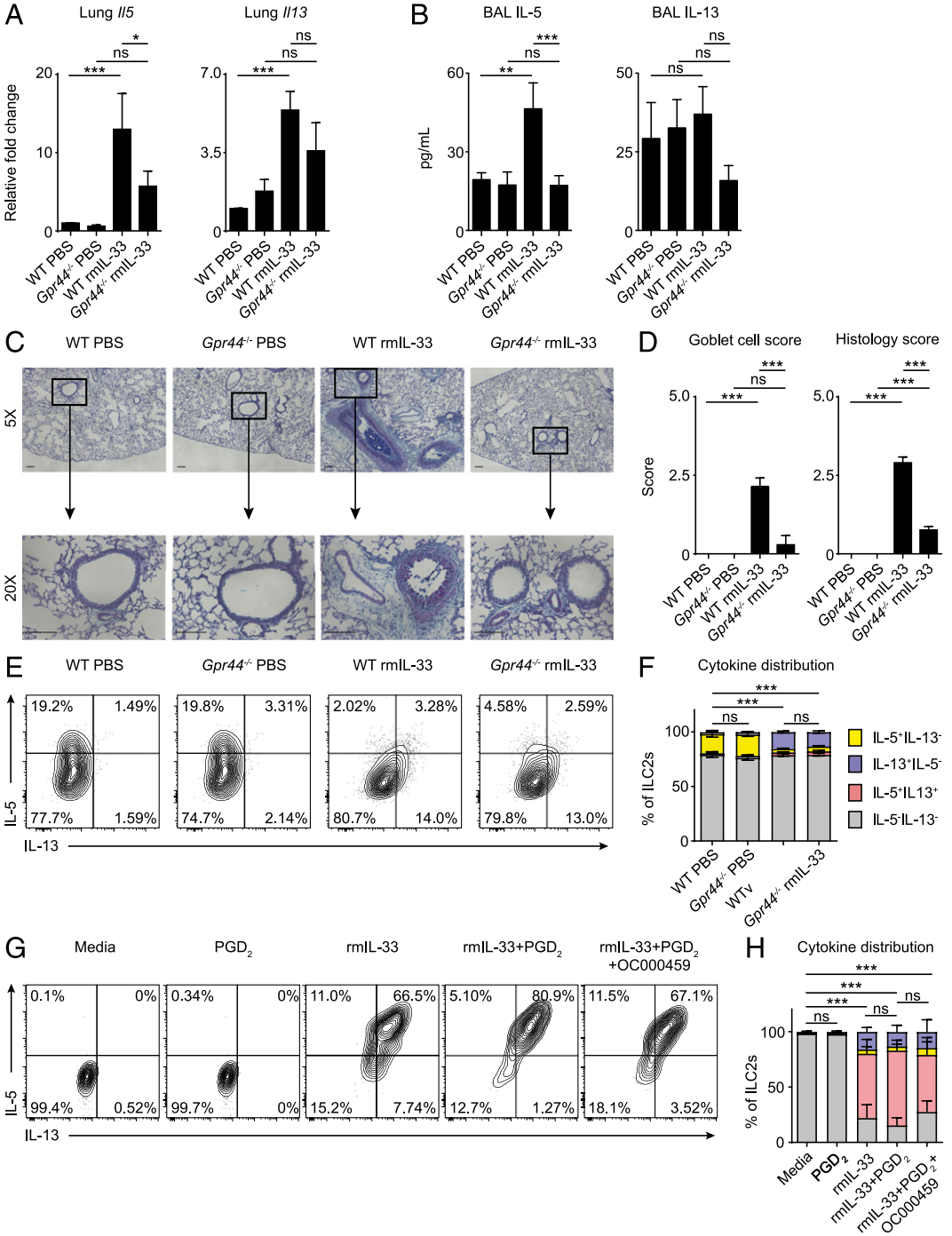

FIGURE 3. CRTH2 deficiency following systemic, ongoing IL-33 administration in vivo affects type 2 cytokine production. C57BL/6 WT and CRTH2-deficient (*Gpr44*$^{-/-}$) mice were treated i.p. three times with 250 ng of rmIL-33 or PBS every other day. On day 6 posttreatment initiation, mice were euthanized, and tissues were collected. Expression of (**A**) *Il5* and *Il13* in lung homogenates as measured by real-time PCR, relative to *Act*β and normalized to WT treated with PBS. (**B**) IL-5 and IL-13 protein levels in the BAL measured by ELISA. (**C**) Representative histological sections of lung stained with PAS/Alcian blue (scale bar, 50 μm) used for (**D**) goblet cell scoring and overall histology scoring reflecting expansion of bronchial-associated lymphoid tissues, lymphoid infiltration around the blood vessels, number of submucosal glands, and accumulation of macrophages/multinucleated giant cells averaged on a per sample basis. (**E**) Representative plots and calculated (**F**) distribution of IL-5 and IL-13 production by lung ILC2s ex vivo following 6-h incubation with BFA as measured by intracellular cytokine staining. (**G**) Representative plots and calculated (**H**) distribution of IL-5 and IL-13 production by lung ILC2s sort-purified from IL-7 complex–treated C57BL/6 WT mice stimulated with 30 ng/ml rmIL-33, 100 nM PGD_2, and/or 1 μM OC000459 following 4-h incubation with BFA, as measured by intracellular cytokine staining. Data are mean ± SEM, analyzed using a linear fixed effect model with pairwise comparison; (A) four independent experiments, (B) two independent experiments, (C)–(F) two independent experiments and (G) and (H) two to four independent experiments; (A) PBS ($n = 4$), rmIL-33 ($n = 8$–9); (B) PBS ($n = 4$), rmIL-33 ($n = 6$); (C) and (D) PBS ($n = 4$), rmIL-33 ($n = 6$); (E) and (F) PBS ($n = 4$), rmIL-33 ($n = 8$–9); (G) and (H) media ($n = 4$), PGD_2 ($n = 4$), IL-33 ($n = 4$), IL-33 plus PGD_2, IL-33 plus PGD_2 plus OC000459 ($n = 2$). $^*p \leq 0.05$, $^{***}p \leq 0.001$; significance shown in (H) is for multiple comparisons for the IL-5$^+$IL-13$^+$ group alone.

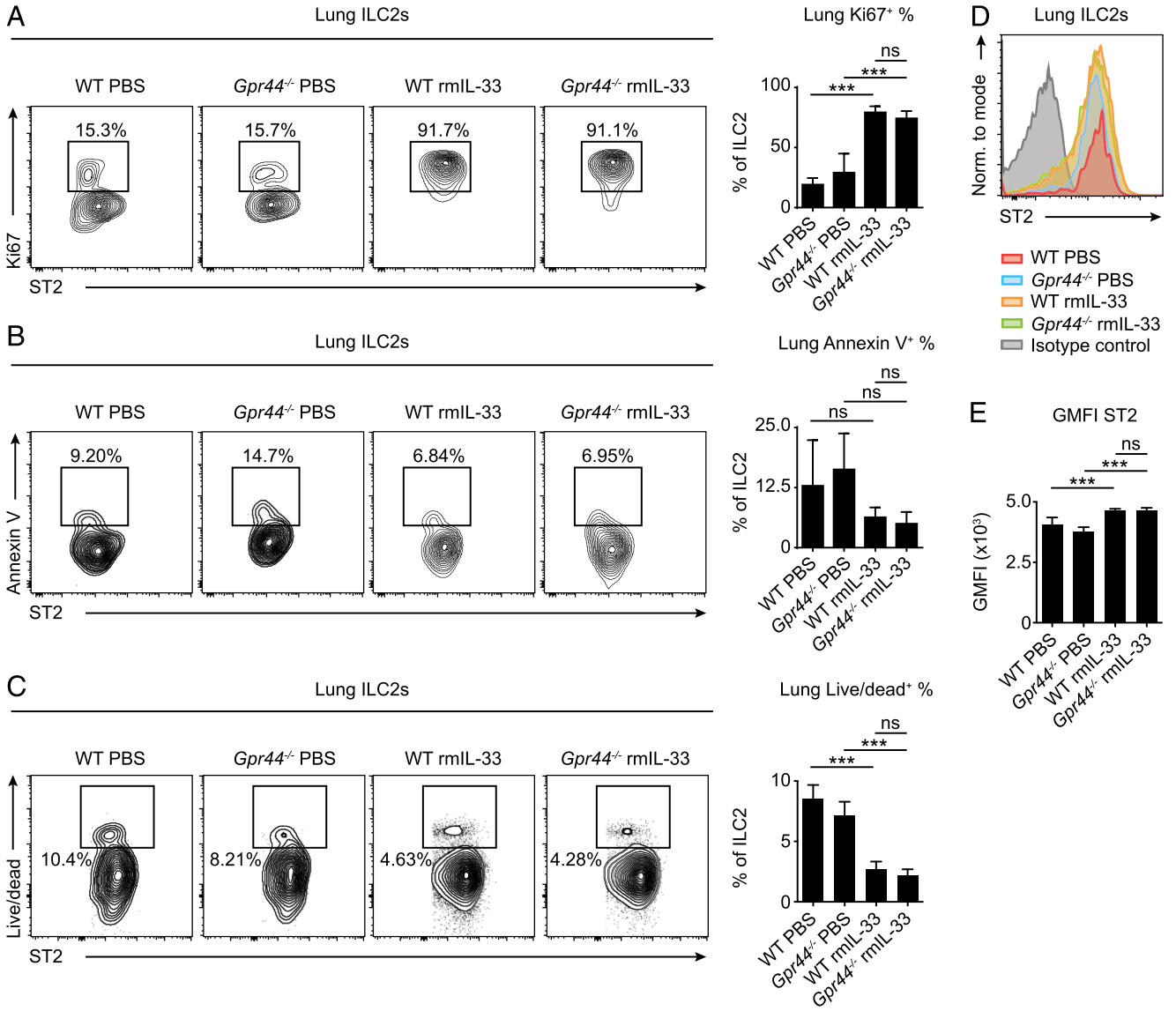

FIGURE 4. CRTH2 does not regulate ILC2 proliferation, apoptosis, cell death, or expression of ST2 following multiple systemic rmIL-33 treatments. C57BL/6 WT and CRTH2-deficient (*Gpr44*$^{-/-}$) mice were treated i.p. three times with 250 ng rmIL-33 or PBS every other day. On day 6 posttreatment initiation, mice were euthanized, and tissues were collected. Percentage of (**A**) Ki67$^+$, (**B**) annexin V$^+$, and (**C**) dead ILC2s in the lung. (**D**) Representative histograms and (**E**) GMFI of ST2 on lung ILC2s. Data are mean ± SEM, analyzed using a linear fixed effect model with pairwise comparison, compiled from three to four independent experiments. (A–C and E) PBS (n = 4–6), rmIL-33 (n = 9–10). ***$p \leq 0.001$.

with recently published studies suggesting that there is a minimal contribution of BM ILC2Ps to seeding tissues during helminth-induced type 2 inflammation (14). Notably, there was a significant decrease in the rmIL-33–elicited percentage of matured ILC2s in the BM of *Gpr44*$^{-/-}$ mice compared with WT mice (Fig. 5C). These data suggest that there is a possible role for CRTH2 in the recirculation of matured KLRG1$^+$ LSIG ILC2s through the BM in response to ongoing administration of rmIL-33 i.p., although these data do not reveal whether this effect is due to effects on differentiation of ILC2s from ILC2Ps.

CRTH2 regulates migration of ILC2s to the lung in response to ongoing i.p. rmIL-33 treatment

Our data suggest that CRTH2 regulates pulmonary ILC2 accumulation during systemic, ongoing rmIL-33 treatment, independent of effects on ILC2 proliferation, apoptosis, or expression of assessed integrins and chemokine receptors, but possibly associated with altered recirculation through the BM. Additionally, our data show that CRTH2 does not impact ILC2 accumulation in the draining MSLN following systemic, ongoing rmIL-33 treatment (Fig. 2E). Together, these data suggest a role for CRTH2 in directly promoting ILC2 migration to or retention in the lung in response to multiple i.p. rmIL-33 treatments (6, 38–40, 42). Furthermore, the lack of deficiency in rmIL-33–elicited ILC2 accumulation in the MSLN in *Gpr44*$^{-/-}$ mice suggests that there may be a CRTH2-dependent signal that controls ILC2 transit from the MSLN to the lung. Thus, we tested whether CRTH2 expression affected the ability of adoptively transferred MSLN ILC2s to accumulate in the lung following IL-33 treatment in a competitive environment. Total cells from the MSLN of congenically marked WT or *Gpr44*$^{-/-}$ mice treated with multiple i.p. rmIL-33 doses were isolated, mixed in a 50:50 ratio, and transferred into congenically disparate WT recipients (resulting in three different identifiable ILC2 populations: recipient, donor WT, and donor *Gpr44*$^{-/-}$) (Fig. 6A). Next, the distribution of genotypes of donor ILC2s (Fig. 6B) that accumulated in recipient tissues following multiple i.p. rmIL-33 treatments was quantified. Congenically disparate donor cells were not detected in mice that did not receive

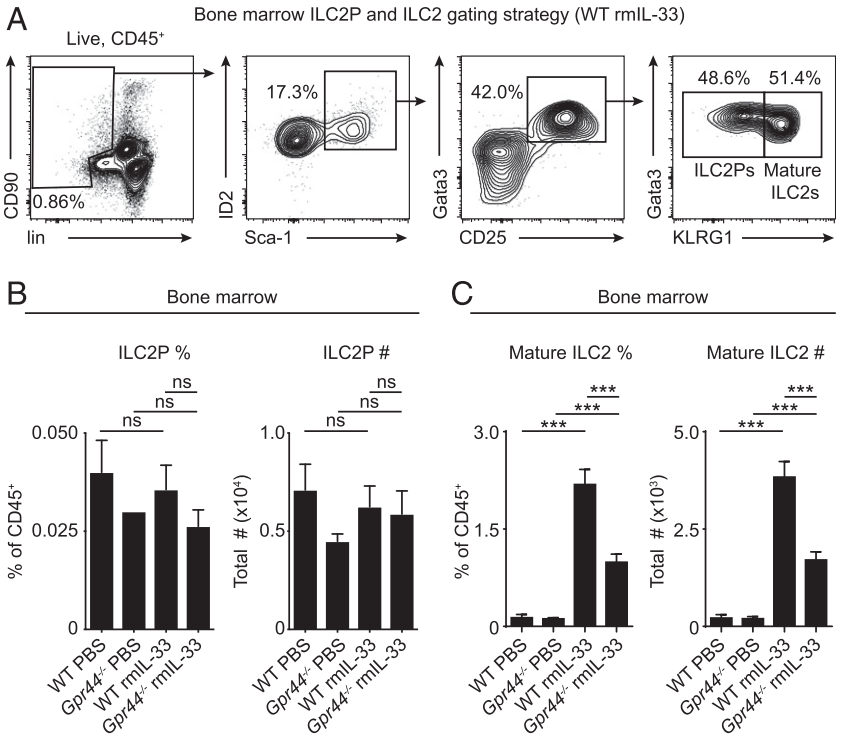

FIGURE 5. CRTH2 regulates the proportion and number of matured ILC2s in BM following multiple systemic rmIL-33 treatments. C57BL/6 WT and CRTH2-deficient (*Gpr44*$^{-/-}$) mice were treated i.p. three times with 250 ng of rmIL-33 or PBS every other day. On day 6 posttreatment initiation, mice were euthanized, and tissues were collected. (**A**) BM ILC2Ps and matured ILC2s were gated as live, CD45$^+$lin$^-$(CD3/CD5/CD11b/CD11c/CD19/NK1.1) LSIG and KLRG1$^+$ LSIG, respectively. (**B**) ILC2P percentage of CD45$^+$ cells and total ILC2P number. (**C**) Mature ILC2 percentage of CD45$^+$ cells and total matured ILC2 number. Data are mean ± SEM, analyzed using a linear fixed effect model with pairwise comparison; data are compiled from three independent experiments; PBS (n = 6), rmIL-33 (n = 8–9). ***$p \leq 0.001$.

a transfer (Supplemental Fig. 4A). Analysis of recipient mice that received a transfer revealed that WT donor ILC2s accumulated significantly more efficiently in the lung and blood than donor *Gpr44*$^{-/-}$ ILC2s (Fig. 6C, 6D). Notably, there was no difference in the percentage of WT versus *Gpr44*$^{-/-}$ donor ILC2s found in the lung-draining MSLN of WT recipient mice treated with multiple i.p. rmIL-33 doses (Fig. 6C, 6D). In addition, there was no difference in the accumulation of WT versus *Gpr44*$^{-/-}$ donor total CD90$^+$ cells or CD4$^+$ T cells in the lung, MSLN, or blood (Supplemental Fig. 4B, 4C). Together, these data suggest that the requirement for CRTH2 in mediating optimal ILC2 accumulation is specific to ILC2s that accumulate in the lung and in the blood and that ILC2s may transit through the MSLN prior to entering the lung in response to prolonged systemic rmIL-33–induced type 2 inflammation.

Discussion

During allergy and helminth infection, ILC2s accumulate at sites of type 2 inflammation and contribute to the clinical manifestations of helminth infection and allergic disease (7, 21, 57). During these diseases, IL-33 and PGD_2 levels are elevated (25, 30, 31, 58–60) and may mediate ILC2 proliferation (8, 13) and migration (6, 40, 42, 49). Some previous work has suggested that ILC2s are largely tissue-resident cells, seeded early in life, that do not migrate between tissues to a substantial degree in adults (8, 13, 14). However, other studies indicate that ILC2s can traffic between tissues in certain contexts (6, 8, 15–19). Thus, it is not clear how ILC2 migration, proliferation, death, chemokine responsiveness, and differentiation contribute to ILC2 accumulation in tissues during type 2 inflammation and, specifically, how IL-33 and the PGD_2–CRTH2 pathway regulate this process.

In this study, using CRTH2-deficient mice, we demonstrate that multiple systemic treatments with rmIL-33 mediated ILC2 expansion during type 2 inflammation, partially dependent on CRTH2 (Fig. 2). We and others have previously reported a key role for CRTH2 in regulating ILC2 accumulation in tissues in vivo and migration in vitro (6, 40, 42), with differential expression of CRTH2 by ILC2s at different tissues sites (6). Specifically, lung ILC2s had a limited migratory potential in response to PGD_2 in vitro, whereas peripheral ILC2s migrated more efficiently (6). Thus, partially CRTH2-dependent IL-33–elicited lung ILC2 accumulation may be mediated by a CRTH2-dependent migratory activity of ILC2s located at distant tissue sites that infiltrate the lung.

Our observations support previous in vitro findings showing a role for IL-33 in the production and release of PGD_2 (36, 37). Consistent with these findings, we show that IL-33 treatment in vivo leads to gene expression of certain enzymes in the PGD_2 synthesis cascade in the lungs and MSLN (Fig. 1, Supplemental Fig. 1A, 1B). However, at the time point assessed, not all components of the PGD_2 synthesis pathway were transcriptionally upregulated, possibly because of the timing of PGD_2 production following initiation of IL-33 treatment, which could result in activation negative feedback loops in vivo that shut down Cox-dependent pathways (61–63). Overall, further experiments that go beyond analysis of gene transcription of PGD_2 synthesis-associated enzymes, including mass spectrometry–based PGD_2 detection in various tissues and throughout a time course of IL-33 treatment will be required to dissect the timing, location, and cellular source of PGD_2 release in vivo following IL-33 stimulation.

The specificity of partially CRTH2-dependent IL-33–elicited cell accumulation in vivo to ILC2s compared with eosinophils and CD4$^+$ T cells that express CRTH2 (20, 39, 45, 46) (Supplemental Fig. 1G–I) speaks to the complexity of the type 2 inflammatory milieu in vivo. Our data support previous findings describing normal eosinophil responses in CRTH2-deficient mice during inflammation (64). Although increased IL-5 levels in CRTH2-deficient mice have been proposed as an explanation for such findings, we find that CRTH2-deficient mice have decreased *Il5* expression in the lung (Fig. 3A) and IL-5 levels in the BAL (Fig. 3B) in our model, associated with a decreased accumulation of lung ILC2s, and no defect in ILC2 IL-5 and IL-13 production ex vivo. In addition, although ILC2 responses can affect the accumulation and function of eosinophils (65–68) and CD4$^+$ T cells (69, 70),

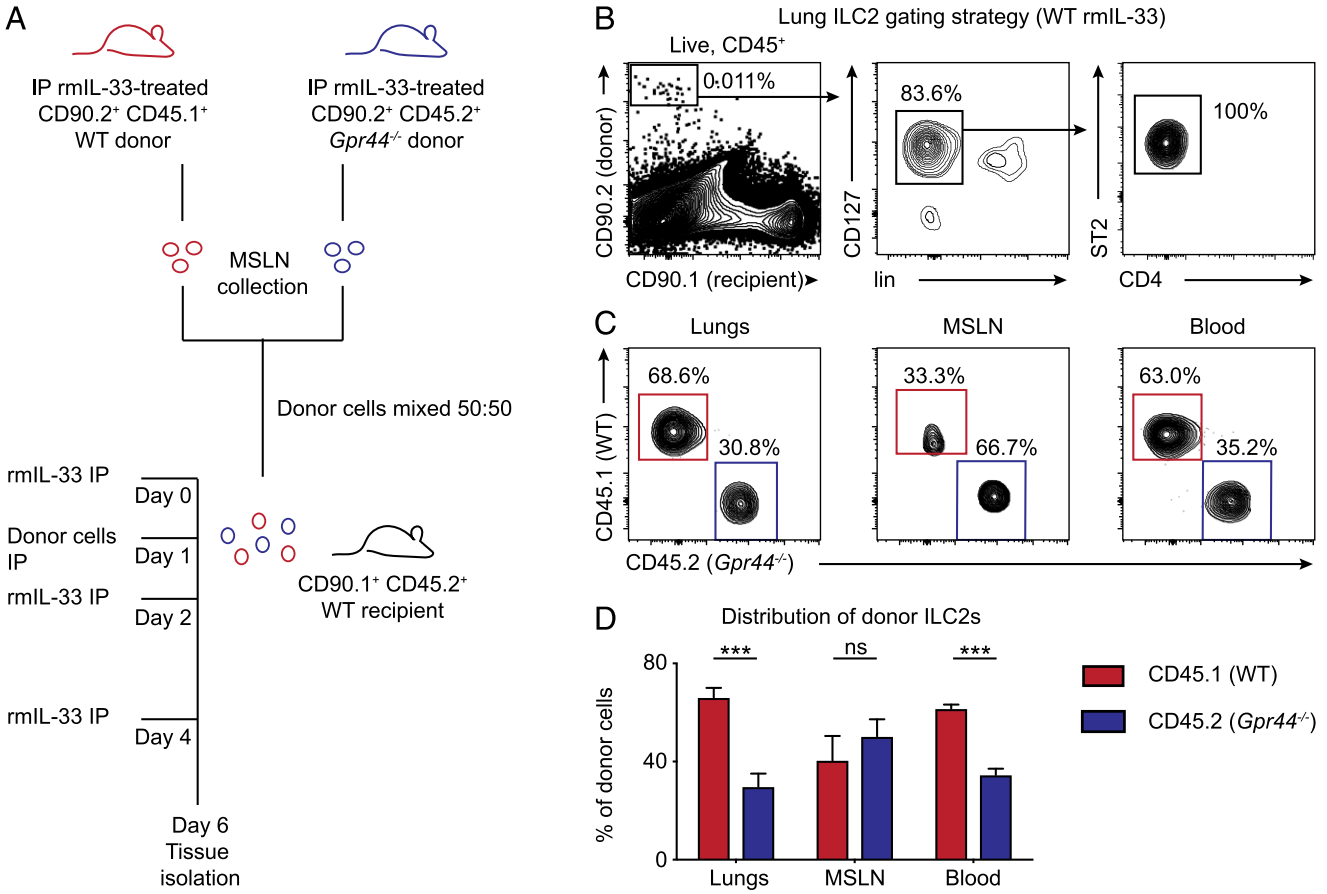

FIGURE 6. CRTH2 regulates accumulation of transferred ILC2s in the lungs in response to ongoing i.p. rmIL-33 treatment. (**A**) MSLN cells from WT and CRTH2-deficient ($Gpr44^{-/-}$) i.p. rmIL-33–treated mice were combined in a 50:50 equal ratio (4×10^5 total) and adoptively transferred i.p. into WT recipient mice that were treated i.p. three times with 250 ng of rmIL-33 every other day (with transfer occurring on day 1 of the regimen). On day 6 posttreatment initiation, mice were euthanized, and tissues were collected. (**B**) Donor ILC2s (identified as $CD45^+CD90^+CD127^+ST2^+CD4^-$) and (**C**) representative and (**D**) average percentages of each genotype in the lungs, MSLN, and blood were determined by flow cytometry. Data are mean ± SEM, analyzed using a linear fixed effect model with pairwise comparison; data are compiled from two independent experiments; PBS ($n = 4$), rmIL-33 ($n = 6$). $^{***}p \leq 0.001$.

eosinophils and T cells can also be directly regulated by IL-33 via expression of ST2 (20, 71) or indirectly by IL-33–mediated activation of other regulatory and/or adhesion factors (72–74). Furthermore, despite normal eosinophil and $CD4^+$ T cell responses and intact IL-5 and IL-13 production capacity in lung ILC2s (Fig. 3E, 3F) in CRTH2-deficient mice following ongoing, systemic IL-33 treatment, partial abrogation of ILC2 accumulation in $Gpr44^{-/-}$ mice was still associated with a decrease in the magnitude of type 2 inflammatory signatures in the lung, as measured by histological analysis (Fig. 3C, 3D). This may be the case because of the residence of ILC2 in perivascular niches close to bronchi and blood vessels (74, 75), where they could have direct effects on inflammatory responses in the tissue. Further studies will be required to assess how IL-33 and the PGD_2–CRTH2 pathway regulate tissue accumulation and cytokine production from a network of ILC2s and other immune and stromal cell types to promote type 2 inflammation.

Critically, our results using various modes and routes of IL-33 delivery and stimulation of type 2 inflammation provide a new dimension to the ongoing debate about ILC2 tissue residency (8, 13, 14, 76) and circulation (18). Our data show that lung ILC2 accumulation in response local IN IL-33 delivery, which would mostly influence expansion of tissue-resident ILC2s, is not dependent on CRTH2, whereas lung ILC2 accumulation in response to systemic i.p. delivery, which would stimulate ILC2s and ILC2 progenitors at different tissue sites, is partially CRTH2 dependent. The absence of an effect of CRTH2 on ILC2 accumulation in response to prolonged local delivery of IL-33, acute administration of IL-33, and acute lung inflammation on day 2 after *N. brasiliensis* infection support studies that show that ILC2s do not migrate across a parabiont pair in response to IN IL-33 delivery (13). These data emphasize the chemotactic role of the PGD_2–CRTH2 pathway during systemic, ongoing IL-33–induced type 2 inflammation yet also support previous studies that suggest that IL-33–mediated ILC2 expansion is dependent on multiple pathways (11, 16, 17, 51). Critically, multiple pathways and mechanisms clearly regulate ILC2 accumulation in the lung in response to IL-33, regardless of route or timing of administration, as we observe a partial but not total abrogation of systemic IL-33–elicited ILC2 accumulation in CRTH2-deficient mice. The ability of IL-33 to promote some accumulation of ILC2s in the lung in the absence of CRTH2 could be due to the activation of other trafficking pathways (11, 16, 17, 51, 74) or could be a result of the ability of IL-33 to act directly on ILC2s to promote proliferation (16, 77, 78) or survival (29). Together, our data and recent literature suggest that the timing and distribution of release of activating cytokines, such as IL-33, may dictate the factors that control the recruitment and circulation of ILC2s from other tissue sites.

Notably, it remains unclear how and from where ILC2s traffic to access the lungs during prolonged systemic type 2 inflammation in

adult mice. In an adoptive transfer model, we show that ILC2s isolated from the MSLN injected i.p. into WT mice treated with multiple i.p. doses of rmIL-33 had migratory potential to the lung that was dependent on CRTH2 but that accumulation in the original tissue, the MSLN, was not impacted by CRTH2 (Fig. 6C, 6D). These findings suggest that ILC2s can migrate to and also from LNs, an idea that is supported by recent studies that used the Kaede photoconvertible mouse model to provide evidence for the presence of migratory ILC2 in peripheral LNs (79). Taken together, these data (79) and our findings suggest that ILC2s that accumulate in the lung following ongoing i.p. rmIL-33 treatment may traffic through the lung-draining MSLN prior to entering the lung or being retained there. However, questions remain as to whether CRTH2 regulates the recirculation of multipotential inflammatory KLRG1^{+}ST2^{-} ILC2s from the gut or another tissues that then accumulate in the lung (15, 18) following prolonged IL-33 stimulation.

Elevated plasma levels of IL-33 have been reported in various human disease conditions, including allergic lung asthma (25, 58–60), in which ILC2s are known to play a significant role (80, 81). In addition, CRTH2 inhibitors can decrease signs and symptoms of allergic lung inflammation in certain patient cohorts but not all individuals (82–84). Therefore, a better understanding of how the IL-33 and PGD_2–CRTH2 pathways intersect to promote ILC2 population expansion through proliferation and interorgan trafficking and function of ILC2s in the lung is critical to understanding how CRTH2 inhibitors and other inhibitors that regulate ILC2s could be effectively deployed to alleviate allergic lung inflammation in different human patient populations (82–84). Although additional studies using human patient samples will be required to test the role of CRTH2 in various human disease states, our study suggests that CRTH2 inhibitors may be more effective clinically in the context of type 2 inflammation associated with prolonged and systemic IL-33 stimulation.

Acknowledgments

We thank members of the Tait Wojno, Rudd, and von Moltke laboratories and participants in the Cornell College of Veterinary Medicine Leadership Program for input during project design and manuscript development. We also thank Adam Wojno, Carol Bayles, Rebecca Williams, Chris Donohue, and the Cornell University Biomedical Sciences Flow Cytometry Core and the Biotechnology Resource Center Imaging Core for cell sorting and assistance with flow cytometry and Lynn Johnson from the Cornell Statistical Consulting Unit for advice on statistical analysis.

Disclosures

The authors have no financial conflicts of interest.

References

1. Neill, D. R., S. H. Wong, A. Bellosi, R. J. Flynn, M. Daly, T. K. Langford, C. Bucks, C. M. Kane, P. G. Fallon, R. Pannell, et al. 2010. Nuocytes represent a new innate effector leukocyte that mediates type-2 immunity. *Nature* 464: 1367–1370.
2. Price, A. E., H. E. Liang, B. M. Sullivan, R. L. Reinhardt, C. J. Eisley, D. J. Erle, and R. M. Locksley. 2010. Systemically dispersed innate IL-13-expressing cells in type 2 immunity. *Proc. Natl. Acad. Sci. USA* 107: 11489–11494.
3. Kim, B. S., E. D. T. Wojno, and D. Artis. 2013. Innate lymphoid cells and allergic inflammation. *Curr. Opin. Immunol.* 25: 738–744.
4. Mjösberg, J. M., S. Trifari, N. K. Crellin, C. P. Peters, C. M. van Drunen, B. Piet, W. J. Fokkens, T. Cupedo, and H. Spits. 2011. Human IL-25- and IL-33-responsive type 2 innate lymphoid cells are defined by expression of CRTH2 and CD161. *Nat. Immunol.* 12: 1055–1062.
5. Walker, J. A., J. L. Barlow, and A. N. J. McKenzie. 2013. Innate lymphoid cells--how did we miss them? *Nat. Rev. Immunol.* 13: 75–87.
6. Wojno, E. D., L. A. Monticelli, S. V. Tran, T. Alenghat, L. C. Osborne, J. J. Thome, C. Willis, A. Budelsky, D. L. Farber, and D. Artis. 2015. The prostaglandin D_2 receptor CRTH2 regulates accumulation of group 2 innate lymphoid cells in the inflamed lung. *Mucosal Immunol.* 8: 1313–1323.
7. Tait Wojno, E. D., and D. Artis. 2016. Emerging concepts and future challenges in innate lymphoid cell biology. *J. Exp. Med.* 213: 2229–2248.
8. Gasteiger, G., X. Fan, S. Dikiy, S. Y. Lee, and A. Y. Rudensky. 2015. Tissue residency of innate lymphoid cells in lymphoid and nonlymphoid organs. *Science* 350: 981–985.
9. Mindt, B. C., J. H. Fritz, and C. U. Duerr. 2018. Group 2 innate lymphoid cells in pulmonary immunity and tissue homeostasis. *Front. Immunol.* 9: 840.
10. Klein Wolterink, R. G., A. Kleinjan, M. van Nimwegen, I. Bergen, M. de Bruijn, Y. Levani, and R. W. Hendriks. 2012. Pulmonary innate lymphoid cells are major producers of IL-5 and IL-13 in murine models of allergic asthma. *Eur. J. Immunol.* 42: 1106–1116.
11. Oczypok, E. A., P. S. Milutinovic, J. F. Alcorn, A. Khare, L. T. Crum, M. L. Manni, M. W. Epperly, A. M. Pawluk, A. Ray, and T. D. Oury. 2015. Pulmonary receptor for advanced glycation end-products promotes asthma pathogenesis through IL-33 and accumulation of group 2 innate lymphoid cells. *J. Allergy Clin. Immunol.* 136: 747–756.e4.
12. Yasuda, K., T. Muto, T. Kawagoe, M. Matsumoto, Y. Sasaki, K. Matsushita, Y. Taki, S. Futatsugi-Yumikura, H. Tsutsui, K. J. Ishii, et al. 2012. Contribution of IL-33-activated type II innate lymphoid cells to pulmonary eosinophilia in intestinal nematode-infected mice. *Proc. Natl. Acad. Sci. USA* 109: 3451–3456.
13. Moro, K., H. Kabata, M. Tanabe, S. Koga, N. Takeno, M. Mochizuki, K. Fukunaga, K. Asano, T. Betsuyaku, and S. Koyasu. 2016. Interferon and IL-27 antagonize the function of group 2 innate lymphoid cells and type 2 innate immune responses. *Nat. Immunol.* 17: 76–86.
14. Schneider, C., J. Lee, S. Koga, R. R. Ricardo-Gonzalez, J. C. Nussbaum, L. K. Smith, S. A. Villeda, H. E. Liang, and R. M. Locksley. 2019. Tissue-resident group 2 innate lymphoid cells differentiate by layered ontogeny and in situ perinatal priming. *Immunity* 50: 1425–1438.e5.
15. Huang, Y., K. Mao, X. Chen, M. A. Sun, T. Kawabe, W. Li, N. Usher, J. Zhu, J. F. Urban, Jr., W. E. Paul, and R. N. Germain. 2018. S1P-dependent interorgan trafficking of group 2 innate lymphoid cells supports host defense. *Science* 359: 114–119.
16. Stier, M. T., J. Zhang, K. Goleniewska, J. Y. Cephus, M. Rusznak, L. Wu, L. Van Kaer, B. Zhou, D. C. Newcomb, and R. S. Peebles, Jr. 2018. IL-33 promotes the egress of group 2 innate lymphoid cells from the bone marrow. *J. Exp. Med.* 215: 263–281.
17. Karta, M. R., P. S. Rosenthal, A. Beppu, C. Y. Vuong, M. Miller, S. Das, R. C. Kurten, T. A. Doherty, and D. H. Broide. 2018. β_2 integrins rather than β_1 integrins mediate Alternaria-induced group 2 innate lymphoid cell trafficking to the lung. *J. Allergy Clin. Immunol.* 141: 329–338.e12.
18. Huang, Y., L. Guo, J. Qiu, X. Chen, J. Hu-Li, U. Siebenlist, P. R. Williamson, J. F. Urban, Jr., and W. E. Paul. 2015. IL-25-responsive, lineage-negative KLRG1(hi) cells are multipotential 'inflammatory' type 2 innate lymphoid cells. *Nat. Immunol.* 16: 161–169.
19. Germain, R. N., and Y. Huang. 2019. ILC2s - resident lymphocytes pre-adapted to a specific tissue or migratory effectors that adapt to where they move? *Curr. Opin. Immunol.* 56: 76–81.
20. Oyesola, O. O., S. P. Früh, L. M. Webb, and E. D. Tait Wojno. 2018. Cytokines and beyond: regulation of innate immune responses during helminth infection. *Cytokine*. pii: S1043–4666(18)30356–9.
21. Vivier, E., D. Artis, M. Colonna, A. Diefenbach, J. P. Di Santo, G. Eberl, S. Koyasu, R. M. Locksley, A. N. J. McKenzie, R. E. Mebius, et al. 2018. Innate lymphoid cells: 10 years on. *Cell* 174: 1054–1066.
22. Inclan-Rico, J. M., and M. C. Siracusa. 2018. First responders: innate immunity to helminths. *Trends Parasitol.* 34: 861–880.
23. Hung, L. Y., I. P. Lewkowich, L. A. Dawson, J. Downey, Y. Yang, D. E. Smith, and D. R. Herbert. 2013. IL-33 drives biphasic IL-13 production for non-canonical Type 2 immunity against hookworms. *Proc. Natl. Acad. Sci. USA* 110: 282–287.
24. Martin, N. T., and M. U. Martin. 2016. Interleukin 33 is a guardian of barriers and a local alarmin. *Nat. Immunol.* 17: 122–131.
25. Guo, Z., J. Wu, J. Zhao, F. Liu, Y. Chen, L. Bi, S. Liu, and L. Dong. 2014. IL-33 promotes airway remodeling and is a marker of asthma disease severity. *J. Asthma* 51: 863–869.
26. Wills-Karp, M., R. Rani, K. Dienger, I. Lewkowich, J. G. Fox, C. Perkins, L. Lewis, F. D. Finkelman, D. E. Smith, P. J. Bryce, et al. 2012. Trefoil factor 2 rapidly induces interleukin 33 to promote type 2 immunity during allergic asthma and hookworm infection. *J. Exp. Med.* 209: 607–622.
27. Duerr, C. U., C. D. A. McCarthy, B. C. Mindt, M. Rubio, A. P. Meli, J. Pothlichet, M. M. Eva, J. F. Gauchat, S. T. Qureshi, B. D. Mazer, et al. 2016. Type I interferon restricts type 2 immunopathology through the regulation of group 2 innate lymphoid cells. *Nat. Immunol.* 17: 65–75.
28. Molofsky, A. B., F. Van Gool, H. E. Liang, S. J. Van Dyken, J. C. Nussbaum, J. Lee, J. A. Bluestone, and R. M. Locksley. 2015. Interleukin-33 and interferon-γ counter-regulate group 2 innate lymphoid cell activation during immune perturbation. *Immunity* 43: 161–174.
29. Camelo, A., G. Rosignoli, Y. Ohne, R. A. Stewart, C. Overed-Sayer, M. A. Sleeman, and R. D. May. 2017. IL-33, IL-25, and TSLP induce a distinct phenotypic and activation profile in human type 2 innate lymphoid cells. *Blood Adv.* 1: 577–589.
30. Murray, J. J., A. B. Tonnel, A. R. Brash, L. J. Roberts, II, P. Gosset, R. Workman, A. Capron, and J. A. Oates. 1986. Release of prostaglandin D2 into human airways during acute antigen challenge. *N. Engl. J. Med.* 315: 800–804.
31. Fajt, M. L., S. L. Gelhaus, B. Freeman, C. E. Uvalle, J. B. Trudeau, F. Holguin, and S. E. Wenzel. 2013. Prostaglandin D_2 pathway upregulation: relation to asthma severity, control, and TH2 inflammation. *J. Allergy Clin. Immunol.* 131: 1504–1512.
32. Konya, V., and J. Mjösberg. 2016. Lipid mediators as regulators of human ILC2 function in allergic diseases. *Immunol. Lett.* 179: 36–42.

33. Balzar, S., M. L. Fajt, S. A. A. Comhair, S. C. Erzurum, E. Bleecker, W. W. Busse, M. Castro, B. Gaston, E. Israel, L. B. Schwartz, et al. 2011. Mast cell phenotype, location, and activation in severe asthma. Data from the Severe Asthma Research Program. *Am. J. Respir. Crit. Care Med.* 183: 299–309.
34. Joo, M., and R. T. Sadikot. 2012. PGD synthase and PGD2 in immune resposne. *Mediators Inflamm.* 2012: 503128.
35. Kostenis, E., and T. Ulven. 2006. Emerging roles of DP and CRTH2 in allergic inflammation. *Trends Mol. Med.* 12: 148–158.
36. Maric, J., A. Ravindran, L. Mazzurana, A. Van Acker, A. Rao, E. Kokkinou, M. Ekoff, D. Thomas, A. Fauland, G. Nilsson, et al. 2019. Cytokine-induced endogenous production of prostaglandin D_2 is essential for human group 2 innate lymphoid cell activation. *J. Allergy Clin. Immunol.* 143: 2202–2214.e5
37. Moulin, D., O. Donzé, D. Talabot-Ayer, F. Mézin, G. Palmer, and C. Gabay. 2007. Interleukin (IL)-33 induces the release of pro-inflammatory mediators by mast cells. *Cytokine* 40: 216–225.
38. Monneret, G., S. Gravel, M. Diamond, J. Rokach, and W. S. Powell. 2001. Prostaglandin D_2 is a potent chemoattractant for human eosinophils that acts via a novel DP receptor. *Blood* 98: 1942–1948.
39. Hirai, H., K. Tanaka, O. Yoshie, K. Ogawa, K. Kenmotsu, Y. Takamori, M. Ichimasa, K. Sugamura, M. Nakamura, S. Takano, and K. Nagata. 2001. Prostaglandin D2 selectively induces chemotaxis in T helper type 2 cells, eosinophils, and basophils via seven-transmembrane receptor CRTH2. *J. Exp. Med.* 193: 255–261.
40. Xue, L., M. Salimi, I. Panse, J. M. Mjösberg, A. N. J. McKenzie, H. Spits, P. Klenerman, and G. Ogg. 2014. Prostaglandin D2 activates group 2 innate lymphoid cells through chemoattractant receptor-homologous molecule expressed on TH2 cells. *J. Allergy Clin. Immunol.* 133: 1184–1194.
41. Barnig, C., M. Cernadas, S. Dutile, X. Liu, M. A. Perrella, S. Kazani, M. E. Wechsler, E. Israel, and B. D. Levy. 2013. Lipoxin A_4 regulates natural killer cell and type 2 innate lymphoid cell activation in asthma. *Sci. Transl. Med.* 5: 174ra26.
42. Chang, J. E., T. A. Doherty, R. Baum, and D. Broide. 2014. Prostaglandin D2 regulates human type 2 innate lymphoid cell chemotaxis. *J. Allergy Clin. Immunol.* 133: 899–901.e3.
43. Camberis, M., G. Le Gros, and J. Urban. 2003. Animal model of nippostrongylus brasiliensis and heligmosomoides polygyrus. *Curr. Protoc. Immunol.* Chapter 19: Unit 19.12.
44. Pettipher, R., S. L. Vinall, L. Xue, G. Speight, E. R. Townsend, L. Gazi, C. J. Whelan, R. E. Armer, M. A. Payton, and M. G. Hunter. 2012. Pharmacologic profile of OC000459, a potent, selective, and orally active D prostanoid receptor 2 antagonist that inhibits mast cell-dependent activation of T helper 2 lymphocytes and eosinophils. *J. Pharmacol. Exp. Ther.* 340: 473–482.
45. Nagata, K., H. Hirai, K. Tanaka, K. Ogawa, T. Aso, K. Sugamura, M. Nakamura, and S. Takano. 1999. CRTH2, an orphan receptor of T-helper-2-cells, is expressed on basophils and eosinophils and responds to mast cell-derived factor(s). *FEBS Lett.* 459: 195–199.
46. Nagata, K., K. Tanaka, K. Ogawa, K. Kemmotsu, T. Imai, O. Yoshie, H. Abe, K. Tada, M. Nakamura, K. Sugamura, and S. Takano. 1999. Selective expression of a novel surface molecule by human Th2 cells in vivo. *J. Immunol.* 162: 1278–1286.
47. Nagashima, H., T. Mahlakõiv, H. Y. Shih, F. P. Davis, F. Meylan, Y. Huang, O. J. Harrison, C. Yao, Y. Mikami, J. F. Urban, Jr., et al. 2019. Neuropeptide CGRP limits group 2 innate lymphoid cell responses and constrains type 2 inflammation. *Immunity* 51: 682–695.e6.
48. Firestein, G. S. 2012. 47 - mechanisms of inflammation and tissue repair. In *Goldman's Cecil Medicine.* Elsevier, Amsterdam, the Netherlands, p. 230–235.
49. Kim, C. H., S. Hashimoto-Hill, and M. Kim. 2016. Migration and tissue tropism of innate lymphoid cells. *Trends Immunol.* 37: 68–79.
50. Soriani, A., H. Stabile, A. Gismondi, A. Santoni, and G. Bernardini. 2018. Chemokine regulation of innate lymphoid cell tissue distribution and function. *Cytokine Growth Factor Rev.* 42: 47–55.
51. Lei, A. H., Q. Xiao, G. Y. Liu, K. Shi, Q. Yang, X. Li, Y. F. Liu, H. K. Wang, W. P. Cai, Y. J. Guan, et al. 2018. ICAM-1 controls development and function of ILC2. *J. Exp. Med.* 215: 2157–2174.
52. Xue, L., J. Fergusson, M. Salimi, I. Panse, J. E. Ussher, A. N. Hegazy, S. L. Vinall, D. G. Jackson, M. G. Hunter, R. Pettipher, et al. 2015. Prostaglandin D2 and leukotriene E4 synergize to stimulate diverse TH2 functions and TH2 cell/neutrophil crosstalk. *J. Allergy Clin. Immunol.* 135: 1358–66.e1–11.
53. Bar-Ephraim, Y. E., J. J. Koning, E. Burniol Ruiz, T. Konijn, V. P. Mourits, K. A. Lakeman, L. Boon, M. Bögels, J. P. van Maanen, J. M. M. Den Haan, et al. 2019. CD62L is a functional and phenotypic marker for circulating innate lymphoid cell precursors. *J. Immunol.* 202: 171–182.
54. Yoshie, O., and K. Matsushima. 2015. CCR4 and its ligands: from bench to bedside. *Int. Immunol.* 27: 11–20.
55. Hoyler, T., C. S. Klose, A. Souabni, A. Turqueti-Neves, D. Pfeifer, E. L. Rawlins, D. Voehringer, M. Busslinger, and A. Diefenbach. 2012. The transcription factor GATA-3 controls cell fate and maintenance of type 2 innate lymphoid cells. *Immunity* 37: 634–648.
56. Walker, J. A., and A. N. McKenzie. 2013. Development and function of group 2 innate lymphoid cells. *Curr. Opin. Immunol.* 25: 148–155.
57. Webb, L. M., and E. D. Tait Wojno. 2017. The role of rare innate immune cells in Type 2 immune activation against parasitic helminths. *Parasitology* 144: 1288–1301.
58. Raeiszadeh Jahromi, S., P. A. Mahesh, B. S. Jayaraj, S. R. V. Madhunapantula, A. D. Holla, S. Vishweswaraiah, and N. B. Ramachandra. 2014. Serum levels of IL-10, IL-17F and IL-33 in patients with asthma: a case-control study. *J. Asthma* 51: 1004–1013.
59. Bahrami Mahneh, S., M. Movahedi, Z. Aryan, M. A. Bahar, A. Rezaei, M. Sadr, and N. Rezaei; Universal Scientific Education and Research Network (USERN). 2015. Serum IL-33 is elevated in children with asthma and is associated with disease severity. *Int. Arch. Allergy Immunol.* 168: 193–196.
60. Bonanno, A., S. Gangemi, S. La Grutta, V. Malizia, L. Riccobono, P. Colombo, F. Cibella, and M. Profita. 2014. 25-Hydroxyvitamin D, IL-31, and IL-33 in children with allergic disease of the airways. *Mediators Inflamm.* 2014: 520241.
61. Mukherjee, P. K., V. L. Marcheselli, C. N. Serhan, and N. G. Bazan. 2004. Neuroprotectin D1: a docosahexaenoic acid-derived docosatriene protects human retinal pigment epithelial cells from oxidative stress. *Proc. Natl. Acad. Sci. USA* 101: 8491–8496.
62. Wu, D., S. Zheng, W. Li, L. Yang, Y. Liu, X. Zheng, Y. Yang, L. Yang, Q. Wang, F. G. Smith, and S. Jin. 2013. Novel biphasic role of resolvin D1 on expression of cyclooxygenase-2 in lipopolysaccharide-stimulated lung fibroblasts is partly through PI3K/AKT and ERK2 pathways. *Mediators Inflamm.* 2013: 964012.
63. Buckley, C. D., D. W. Gilroy, and C. N. Serhan. 2014. Proresolving lipid mediators and mechanisms in the resolution of acute inflammation. *Immunity* 40: 315–327.
64. Kagawa, S., K. Fukunaga, T. Oguma, Y. Suzuki, T. Shiomi, K. Sayama, T. Kimura, H. Hirai, K. Nagata, M. Nakamura, and K. Asano. 2011. Role of prostaglandin D2 receptor CRTH2 in sustained eosinophil accumulation in the airways of mice with chronic asthma. *Int. Arch. Allergy Immunol.* 155(Suppl. 1) 6–11.
65. Molofsky, A. B., J. C. Nussbaum, H. E. Liang, S. J. Van Dyken, L. E. Cheng, A. Mohapatra, A. Chawla, and R. M. Locksley. 2013. Innate lymphoid type 2 cells sustain visceral adipose tissue eosinophils and alternatively activated macrophages. *J. Exp. Med.* 210: 535–549.
66. Nussbaum, J. C., S. J. Van Dyken, J. von Moltke, L. E. Cheng, A. Mohapatra, A. B. Molofsky, E. E. Thornton, M. F. Krummel, A. Chawla, H. E. Liang, and R. M. Locksley. 2013. Type 2 innate lymphoid cells control eosinophil homeostasis. *Nature* 502: 245–248.
67. Rana, B. M. J., E. Jou, J. L. Barlow, N. Rodriguez-Rodriguez, J. A. Walker, C. Knox, H. E. Jolin, C. S. Hardman, M. Sivasubramaniam, A. Szeto, et al. 2019. A stromal cell niche sustains ILC2-mediated type-2 conditioning in adipose tissue. *J. Exp. Med.* 216: 1999–2009.
68. Van Gool, F., A. B. Molofsky, M. M. Morar, M. Rosenzwajg, H. E. Liang, D. Klatzmann, R. M. Locksley, and J. A. Bluestone. 2014. Interleukin-5-producing group 2 innate lymphoid cells control eosinophilia induced by interleukin-2 therapy. *Blood* 124: 3572–3576.
69. Halim, T. Y. F., B. M. J. Rana, J. A. Walker, B. Kerscher, M. D. Knolle, H. E. Jolin, E. M. Serrao, L. Haim-Vilmovsky, S. A. Teichmann, H. R. Rodewald, et al. 2018. Tissue-restricted adaptive type 2 immunity is orchestrated by expression of the costimulatory molecule OX40L on group 2 innate lymphoid cells. *Immunity* 48: 1195–1207.e6.
70. Mirchandani, A. S., A. G. Besnard, E. Yip, C. Scott, C. C. Bain, V. Cerovic, R. J. Salmond, and F. Y. Liew. 2014. Type 2 innate lymphoid cells drive $CD4^+$ Th2 cell responses. *J. Immunol.* 192: 2442–2448.
71. Hardman, C., and G. Ogg. 2016. Interleukin-33, friend and foe in type-2 immune responses. *Curr. Opin. Immunol.* 42: 16–24.
72. Johnston, L. K., and P. J. Bryce. 2017. Understanding interleukin 33 and its roles in eosinophil development. *Front. Med. (Lausanne)* 4: 51.
73. Alvarez, F., J. H. Fritz, and C. A. Piccirillo. 2019. Pleiotropic effects of IL-33 on CD4+ T cell differentiation and effector functions. *Front. Immunol.* 10: 522.
74. Puttur, F., L. Denney, L. G. Gregory, J. Vuononvirta, R. Oliver, L. J. Entwistle, S. A. Walker, M. B. Headley, E. J. McGhee, J. E. Pease, et al. 2019. Pulmonary environmental cues drive group 2 innate lymphoid cell dynamics in mice and humans. *Sci. Immunol.* 4: eaav7638.
75. Dahlgren, M. W., S. W. Jones, K. M. Cautivo, A. Dubinin, J. F. Ortiz-Carpena, S. Farhat, K. S. Yu, K. Lee, C. Wang, A. V. Molofsky, et al. 2019. Adventitial stromal cells define group 2 innate lymphoid cell tissue niches. *Immunity* 50: 707–722.e6.
76. Fan, X., and A. Y. Rudensky. 2016. Hallmarks of tissue-resident lymphocytes. *Cell* 164: 1198–1211.
77. Hayakawa, H., M. Hayakawa, and S. I. Tominaga. 2016. Soluble ST2 suppresses the effect of interleukin-33 on lung type 2 innate lymphoid cells. *Biochem. Biophys. Rep.* 5: 401–407.
78. Lund, S. J., A. Portillo, K. Cavagnero, R. E. Baum, L. H. Naji, J. H. Badrani, A. Mehta, M. Croft, D. H. Broide, and T. A. Doherty. 2017. Leukotriene C4 potentiates IL-33–Induced group 2 innate lymphoid cell activation and lung inflammation. *J. Immunol.* 199: 1096–1104.
79. Dutton, E. E., D. W. Gajdasik, C. Willis, R. Fiancette, E. L. Bishop, A. Camelo, M. A. Sleeman, M. Coccia, A. M. Didierlaurent, M. Tomura, et al. 2019. Peripheral lymph nodes contain migratory and resident innate lymphoid cell populations. *Sci. Immunol.* 4: eaau8082.
80. Barlow, J. L., and A. N. J. McKenzie. 2014. Type-2 innate lymphoid cells in human allergic disease. *Curr. Opin. Allergy Clin. Immunol.* 14: 397–403.
81. Kabata, H., K. Moro, S. Koyasu, and K. Asano. 2015. Group 2 innate lymphoid cells and asthma. *Allergol. Int.* 64: 227–234.
82. Farne, H., D. J. Jackson, and S. L. Johnston. 2016. Are emerging PGD2 antagonists a promising therapy class for treating asthma? *Expert Opin. Emerg. Drugs* 21: 359–364.
83. Thomson, N. C. 2017. New and developing non-adrenoreceptor small molecule drugs for the treatment of asthma. *Expert Opin. Pharmacother.* 18: 283–293.
84. Santini, G., N. Mores, M. Malerba, C. Mondino, G. Macis, and P. Montuschi. 2016. Investigational prostaglandin D2 receptor antagonists for airway inflammation. *Expert Opin. Investig. Drugs* 25: 639–652.